

Negative Capacitance Enables FinFET Scaling Beyond 3nm Node

Ming-Yen Kao, Harshit Agarwal, Member, IEEE, Yu-Hung Liao, Suraj Cheema, Avirup Dasgupta, Member, IEEE, Pragya Kushwaha, Member, IEEE, Ava Tan, Sayeef Salahuddin, Fellow, IEEE, and Chenming Hu, Life Fellow, IEEE

Abstract—A comprehensive study of the scaling of negative capacitance FinFET (NC-FinFET) is conducted with TCAD. We show that the NC-FinFET can be scaled to “2.1nm node” and almost “1.5nm node” that comes two nodes after the industry “3nm node,” which has 16nm L_g and is the last FinFET node according to the International Roadmap for Devices and Systems (IRDS). In addition, for the intervening nodes, NC-FinFET can meet IRDS I_{on} and I_{off} target at target-beating V_{DD} . The benefits of negative capacitance (NC) include improved subthreshold slope (SS), drain-induced barrier lowering (DIBL), V_t roll-off, transconductance over I_d (G_m/I_d), output conductance over I_d (G_d/I_d), and lower V_{DD} . Further scaling may be achieved by improving capacitance matching between ferroelectric (FE) and dielectric (DE).

Index Terms—Scaling, International Roadmap for Devices and Systems (IRDS), Landau equation, negative capacitance field-effect capacitance (NCFET), TCAD.¹

I. INTRODUCTION

The negative capacitance field-effect transistor (NCFET) is a promising technology for near future logic devices [1]. SS, DIBL, V_t roll-off, G_m/I_d , and G_d/I_d of the FinFET can be improved by doping Zr into the HfO_2 high- κ gate dielectric [1-2]. The show stopper to scaling of FinFET, according to IRDS, is the difficulty in reduction of fin-thickness (T_{fin}) and reduction of effective oxide thickness (EOT). Our study shows that NC enables FinFET scaling beyond “3nm node” without requiring further thinning of T_{fin} and gate stack. The scalability of the metal-ferroelectric-metal-insulator-semiconductor (MFMS) NCFET (with internal metal) has been discussed in [3]. Nevertheless, the electrical characteristics of the metal-ferroelectric-insulator-semiconductor (MFIS) NCFET (without internal metal) is different from the MFMS NCFET [4], and an internal metal is not desirable in practical logic devices. In this paper, the scalability of MFIS NC-FinFET will be discussed. Moreover, the parameters of FE used in this paper are extracted from MFIS capacitor, not from the polarization-electric field (PE) loop of metal-ferroelectric-metal (MFM) structure. The extracted FE parameters are experimentally available and ready for MFIS NCFET.

¹ This work was supported by the Berkeley Device Modeling Center, University of California at Berkeley, CA 94720 USA. (Corresponding author: Ming-Yen Kao)

M.-Y. Kao, Y.-H. Liao, S. Cheema, A. Dasgupta, P. Kushwaha, A. Tan, S. Salahuddin, and C. Hu are with the Department of Electrical Engineering and

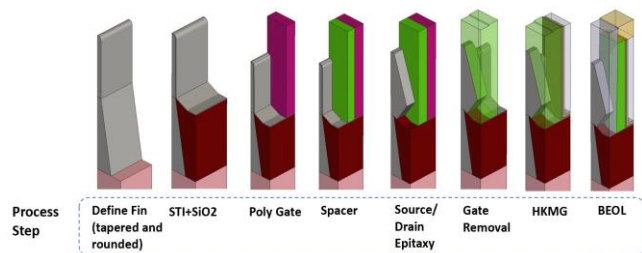


Fig. 1. Process simulation flow. Only the source side half of the FinFET is shown.

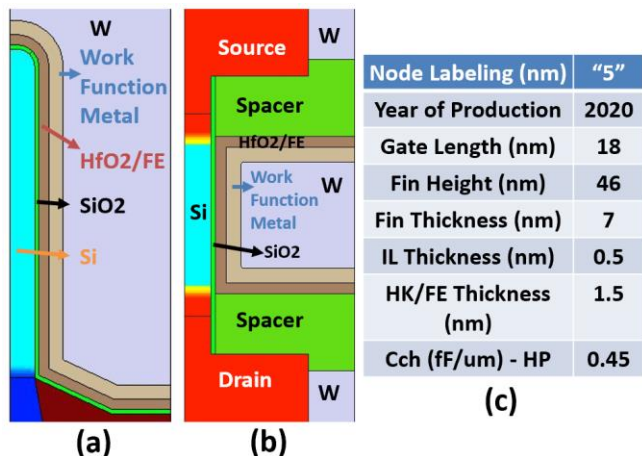


Fig. 2. (a) vertical and (b) horizontal cross sections of the half-FinFET (c) key geometry parameters of the simulated device. Note that the capacitance of the gate stack (C_{ch}) matches with IRDS high performance (HP) requirement, 0.45fF/ μ m.

II. TCAD SIMULATION

Sentaurus Process Simulation [5] is used to build a realistic device for device simulations. The flow of process simulation is shown in Fig. 1. A gate-last process is adopted using a high- κ metal gate. Only the source side of the FinFET is shown for simplicity. Fig. 2 (a) and (b) show the cross-section of the fin. After the device structure is built, Sentaurus Device Simulation [6] is utilized to simulate the electrical characteristics. The electronic band structure with stress effects is included with carrier trajectory and scattering calculations and using the k.p. deformation potential model. Scattering mechanisms such as

Computer Sciences, University of California at Berkeley, Berkeley, CA 94720 USA (e-mail: mingyenkao@berkeley.edu).

H. Agarwal is with Indian Institute of Technology Jodhpur, Karwar, Rajasthan 342037, India.

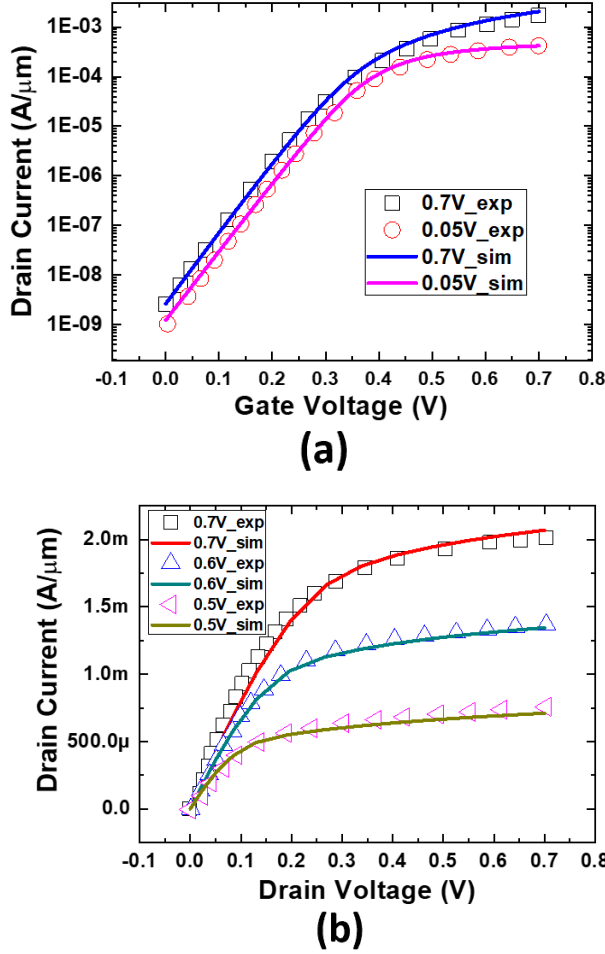


Fig. 3. TCAD FinFET calibration to 18nm L_g Intel experimental data. *Per-foot-print* normalization of I_d is done in this figure to match the Intel presentation. (a) I_d - V_g fitting plot at high and low drain voltage (b) I_d - V_d fitting plot at three different gate voltages, 0.7V, 0.6V, and 0.5V.

phonon scattering, impurity scattering, surface roughness scattering, remote Coulomb scattering, and impact ionization are also included. SRH and Auger recombination are additionally considered. Finally, drift-diffusion with the quantum confinement effect is solved self-consistently with the Sentaurus Device simulator.

An n-type FinFET with fin-height (H_{fin}) of 46nm, T_{fin} of 7nm, and gate length (L_g) of 18nm is calibrated to the “Intel 10nm node” (equivalent to “5nm node” using the IRDS node definition) experimental data [7-8] as shown in Fig. 3. Note that the definition of *per-foot-print* (drain current (I_d) normalized to the fin pitch) is used only in Fig. 3 to match the Intel presentation [7], whereas all other figures and tables on I_d in this paper present I_d *per-channel-width* (I_d normalized to the sum of 2 times H_{fin} plus T_{fin}) because this work is not concerned with fin pitch. After this calibration, all TCAD parameters, including contact resistivity, are fixed, except the change of fin width from 7nm at “5nm node” to 6nm at “3nm node” according to the IRDS definition [8]. The gate stack is composed of a 0.5nm SiO_2 interfacial layer (IL) and either 1.5nm HfO_2 (FinFET) or 1.5nm HZO (NC-FinFET), the latter meaning that HfO_2 is doped with Zr and becomes FE in the NC-

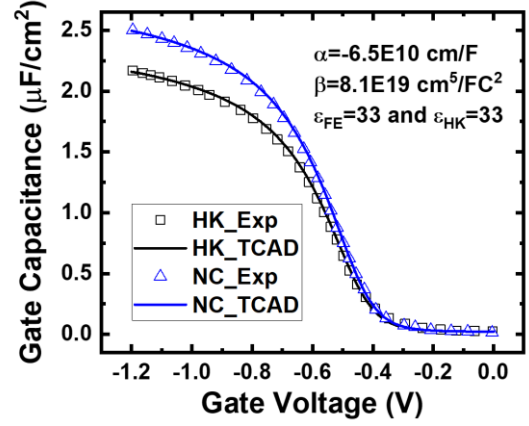


Fig. 4. C-V fitting of the experiment data of NC-MOSCAP. The extracted α and β are equivalent to $P_r = 20 \mu C/cm^2$ and $E_c = 1MV/cm$.

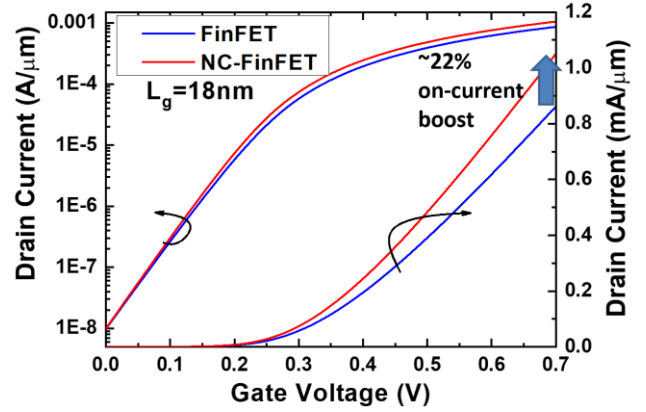


Fig. 5. I_d - V_g plot of the FinFET and the NC-FinFET at $L_g=18nm$.

FinFET simulation. In NC-FinFET simulation, FE parameters, including α and β from Landau’s Equation and background dielectric of FE (ϵ_{FE}), are extracted from experimental C-V of NC MFIS structure [9] (see Fig. 4), and strength of the polarization gradient (domain coupling) is set to be $5 \times 10^{-5} cm^3/F$ (on the same order as [10]). In Fig. 4, gate insulator for both HK and NC constitutes of a chemical oxide (8Å) and 2.8nm layer of HfO_2 or HZO. The extracted dielectric constant of HfO_2 (HK) is 33 which corresponds to 1.1 nm EOT gate stack. On the other hand, very high dielectric constant (>100) exceeding theoretical predictions for Hf and Zr-based dielectrics [11-15] is required to fit the HZO C-V, and the anomalous I-V behavior in [9] must be explained by non-linear response of the gate insulator [16]. Therefore, a model with partially active FE layer in HZO is presented in [16] to explain both the C-V and I-V results in [9]. This work adopt the same methodology to use the Landau-Khalatnikov (L-K) model to extract HZO parameters and fit to Fig. 4, with $\alpha = -6.5 \times 10^{10} \frac{cm}{F}$ and $\beta = 8.1 \times 10^{19} \frac{cm^5}{FC^2}$.

III. RESULTS AND DISCUSSION

Fig. 5 demonstrates the improvement from FinFET to NC-FinFET at $L_g=18nm$, and the boost of I_{on} is about 22% when the I_{off} is aligned at 10nA/ μm . Table 1 shows the IRDS scaling targets from “5nm” to “1.5 nm”. The second row shows the year

1	"2018 IRDS" Node	"5"	"3"	"2.1"	"1.5"
2	Year of Production	2020	2022	2025	2028
3	Physical Gate Length (nm)	18	16	14	12
4	Fin Width (nm)	7		6	
5	IRDS Target V _{DD} (V)	0.70		0.65	
6	Ion Target (mA/ μ m)	0.85	0.91	0.82	0.92
7	Ion of FinFET(mA/ μ m)	0.86	0.93	0.75	0.64
8	Ion of NC-FinFET(mA/ μ m)	1.05	1.12	0.93	0.89

Table 1. Simulation plan follows the IRDS 2018 roadmap. Red highlighting of the TCAD results indicate failure to meet the on-current targets at all future nodes.

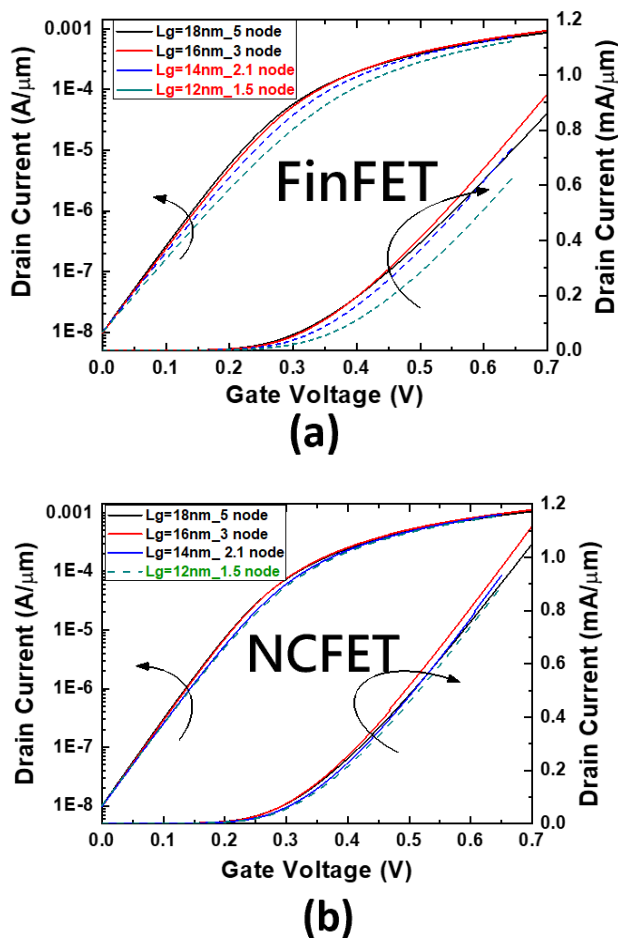


Fig. 6. I_d - V_g of (a) FinFETs and (b) NC-FinFETs with work functions shifted to align the off-current with the IRDS high-performance requirement.

of production [8]. The third row shows the physical gate length. Physical gate length is predicted to reach the scaling limit of 12nm according to IRDS. T_{fin} (the fourth row of Table 1) is set to be 6nm from "3nm" to "1.5nm" according to IRDS definition. The 5th row in Table 1 shows IRDS target V_{DD} , and the 6th row shows the IRDS I_{on} targets at $I_{off} = 10nA/\mu m$. The 7th row shows that simulated FinFETs cannot meet the targets after "3nm node," hence the red color. The 8th row shows that NC-FinFETs with extracted FE parameters can meet IRDS

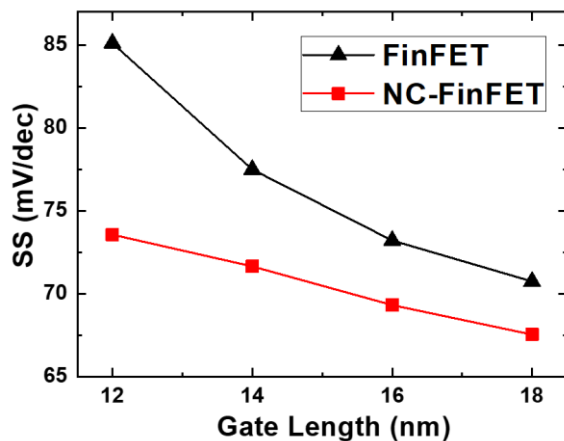


Fig. 7. SS of NC-FinFET is smaller than FinFET at 18nm L_g and rises at lower rate with decreasing L_g .

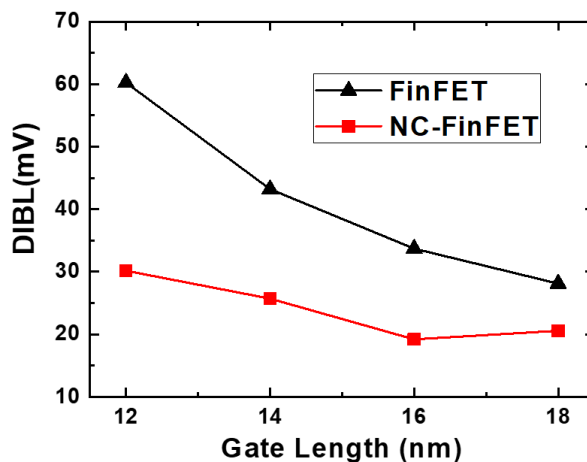


Fig. 8. DIBL versus gate lengths. DIBL is smaller in NC-FinFET and rises at lower rate as L_g shrinks.

requirement one more node beyond "3nm node" and almost meet "1.5nm node" with I_{on} only 3% less than the target I_{on} .

Fig. 6 shows I_d - V_g simulation results at $V_d = IRDS V_{DD}$ from "5nm node" to "1.5nm node" with work function shifted to align the I_{off} at $10nA/\mu m$. One can see that FinFETs beyond "3nm node" cannot meet the IRDS targets in Fig. 6 (a). The nodes which fail to reach the IRDS targets are labeled in red color and plotted in dash line. NC-FinFET, on the other hand, can meet the IRDS targets at "2.1nm node" and almost meet the IRDS target at "1.5nm node" respectively- two more nodes than FinFET in our simulations. The NC-FinFET simulation results are summarized in the 8th row of Table 1. For several nodes, I_{on} is significantly larger than the targets.

SS versus L_g is shown in Fig. 7. SS degrades for both the NC-FinFET and FinFET when L_g decreases, but the SS degrades at a lower rate for the NC-FinFET because the inner-fringing field, which becomes stronger at shorter L_g , helps capacitance matching and enhance V_g -amplification. Note that even if the SS of the NCFET is not below 60mV/dec in the "weak NC" FinFET studied here, the NC effect improves the on/off ratio improvement is large enough to enable 2 more nodes of scaling than simple FinFETs. Fig. 8 shows the DIBL versus different

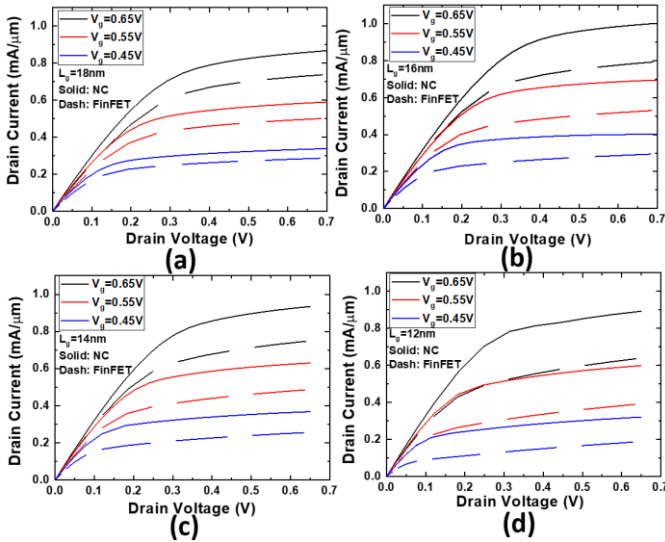


Fig. 9. I_d is larger and g_d is smaller in NC-FinFET than in FinFET at (a). L_g=18nm, at (b) L_g=16nm, at (c) L_g=14nm, and at (d) L_g=12nm.

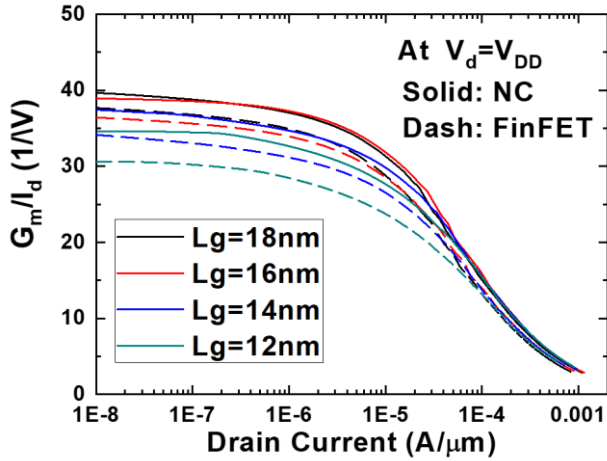


Fig. 10. G_m/I_d versus drain current. NC-FinFETs have better G_m/I_d performance than FinFETs overall.

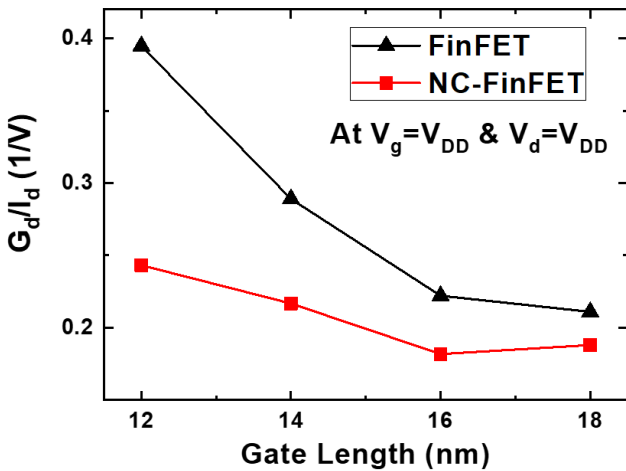


Fig. 11. G_d/I_d versus drain current. NC-FinFET has higher G_m/I_d and lower G_d/I_d leading to better analog performance.

gate length of FinFETs and NC-FinFETs. NC helps relieve the degradation of DIBL, as it can be seen that the slower rate of

"2018 IRDS" Node	"5"	"3"	"2.1"	"1.5"
Year of Production	2020	2022	2025	2028
IRDS Target V _{DD} (V)	0.70	0.69	0.65	0.65
FinFET V _{DD} needed to meet IRDS Target I _{on}	0.70	0.69	X	X
NC-FinFET V _{DD} needed to meet IRDS Target I _{on}	0.63	0.63	0.61	X

Table 2. V_{DD} needed to reach IRDS target on-current (I_{off} is fixed at 10nA/μm) for different IRDS nodes.

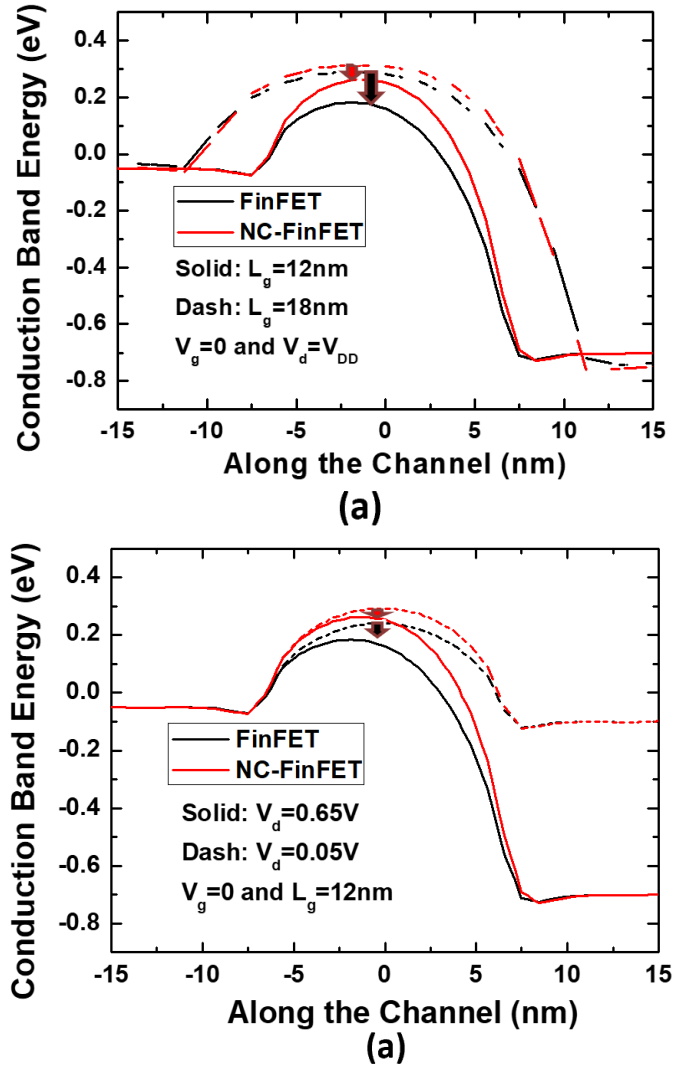


Fig. 12. (a) The potential barrier is higher in NC-FinFET (red) than in FinFET (black), and the difference is larger at L_g=12nm (solid) than at L_g=18nm (dash). (b) DIBL of NC-FinFET is smaller than FinFET. Note that the work function is not shifted in this figure.

increase in DIBL when gate length scales. Note that negative DIBL does not appear because the NC effect is "weak" (only 36% of the HZO is active FE layer) in this extracted parameter set. The SS_{NC}/SS_{FinFET} and DIBL_{NC}/DIBL_{FinFET} trend are consistent with Y. Liao et. al.'s results [17]. Fig. 9 compares the I_d-V_d characteristics of the FinFETs and the NC-FinFETs from L_g=18nm to L_g=12nm. In Fig. 9, NC-FinFETs are plotted in solid lines, and FinFETs are plotted in dash lines. Current of FinFETs decreases a lot from L_g=18nm to L_g=12nm because of the short channel effect; whereas, current of NC-FinFETs barely decreases from L_g=18nm to L_g=12nm.

The scaled NC-FinFETs are also good for analog applications. The g_m/I_d versus I_d of FinFET and NC-FinFET at $L_g=18\text{nm}$, 16nm , 14nm , and 12nm are presented in Fig. 10. The g_m/I_d of the NC-FinFET is better than the conventional FinFET overall, and the g_m/I_d of NC-FinFET at $L_g=18\text{nm}$ and 16nm nearly hit the theoretical limits of 40 1/V at room temperature [18]. The g_d to drain current ratio is shown in Fig. 11. While g_d/I_d increases with shorter channel length for the FinFET due to the short channel effects, the trend of g_d/I_d is the opposite for the NC-FinFET from $L_g=18\text{nm}$ to $L_g=16\text{nm}$ since the FE polarization induced by the inner-fringing field at short L_g and high V_d negates and overwhelms the short channel effect. For NC-FinFET at $L_g=14\text{nm}$ and $L_g=12\text{nm}$, g_d/I_d increase at much slower rate compared with FinFET. This benefits the intrinsic voltage gain, speed of both the static and pass-transistor logic, and noise margin of logic gates [19].

Table 2 shows another way to utilize NC-FinFETs' potential "excess horse power" in the intervening nodes. The V_{DD} of the NC-FinFET is reduced for each L_g by trial and error until I_{on} and I_{off} at $V_d=\text{reduced } V_{DD}$ match the IRDS I_{on} and I_{off} targets, respectively. The reduced (needed) V_{DD} for the scaled NC-FinFET is shown in the last row of Table 2. Some IRDS I_{off} and I_{on} targets may be reachable below the target V_{DD} by 70mV at significant power reduction.

Fig. 12 (a) shows the conduction band energy along the channel at $V_g=0$ and $V_d=V_{DD}$. The black arrow in Fig. 12 (a) demonstrates the reduction of the top-of-barrier (TOB) of FinFETs due to gate length scaling. In comparison, the red arrow in Fig. 12 (a) which indicates the reduction of the TOB in NC-FinFETs due to gate length scaling is much shorter than the black arrow. Fig. 12 (a) shows that NC-FinFETs have better immunity toward gate length scaling. Fig. 12(b) illustrates the reduced drain-induced barrier lowering effects at $L_g=12\text{nm}$. When the inner-fringing field, more significant at high V_d , goes through the channel to the FE film, it induces polarization in the FE such that the NC-FinFETs' channel potential barrier (the red line in Fig. 12 (b)) becomes higher compared with FinFETs' channel potential barrier (the black line in Fig. 12 (b)). That is why the reduction of the TOB due to the increase of drain bias in NC-FinFETs (the red arrow in Fig. 12 (b)) is smaller than the reduction of the TOB of FinFETs (the black arrow in Fig. 12 (b)).

IV. CONCLUSION

NC may enable FinFET scaling 2 nodes beyond the "3nm node" without requiring thinner W_{fin} or high-k film. We note that this is a TCAD simulation study that assumes the uniform FE film which can be scaled from large-area NC-MOSCAP to small NCFET device without changing the properties of the FE film and can be put into production. On the other hand, future HZO optimization with larger portion of active FE layer, multi-layer FEs [20], or varying FE along the channel [21], may lead to even much better NC performance in the future. NC may delay the need for nano-sheet FET in the near term and extend the nanosheet scalability in the long term.

REFERENCES

- [1] S. Salahuddin and S. Datta, "Use of Negative Capacitance to Provide Voltage Amplification for Low Power Nanoscale Devices," *Nano Letters*, vol. 8, no. 2, pp. 405-410, Dec. 2007, doi: 10.1021/nl071804g.
- [2] K.-S. Li, Y.-J. Wei, Y.-J. Chen, W.-C. Chiu, H.-C. Chen, and M.-H. Lee, Y.-F. Chiu, F.-K. Hsueh, B.-W. Wu, P.-G. Chen, T.-Y. Lai, C.-C. Chen, J.-M. Shieh, W.-K. Yeh, S. Salahuddin, and C. Hu, "Negative-Capacitance FinFET Inverter, Ring Oscillator, SRAM Cell, and Ft," in *IEDM Tech Dig.*, Dec. 2018, pp. 31.7.1-31.7.4, doi: 10.1109/IEDM.2018.8614521.
- [3] V. P.-H. Hu, P.-C. Chiu, A. B. Sachid, C. Hu, "Negative capacitance enables FinFET and FDSOI scaling to 2 nm node," in *IEDM Tech Dig.*, Dec. 2017, pp. 23.1.1-23.1.4, doi: 10.1109/IEDM.2017.8268443.
- [4] J. P. Duarte, S. Khandelwal, A. I. Khan, A. Sachid, Y.-K. Lin, H.-L. Chang, S. Salahuddin, and C. Hu, "Compact models of negative-capacitance FinFETs: Lumped and distributed charge models," in *IEDM Tech Dig.*, Dec. 2016 pp. 30.5.1-30.5.4, doi: 10.1109/IEDM.2016.7838514.
- [5] Sentaurus Process User Guide, Version O-2018.06, Synopsys, Mountain View, CA, USA, Sep. 2018.
- [6] Sentaurus Device User Guide, Version O-2018.06, Synopsys, Mountain View, CA, USA, Sep. 2018.
- [7] C. Auth, A. Aliyarukunju, M. Asoro, D. Bergstrom, V. Bhagwat, J. Birdsall, N. Bisnik, M. Buehler, V. Chikarmane, G. Ding, Q. Fu, H. Gomez, W. Han, D. Hanken, M. Haran, M. Hattendorf, R. Heussner, H. Hiramatsu, B. Ho, S. Jaloviar, I. Jin, S. Joshi, S. Kirby, S. Kosaraju, H. Kothari, G. Leatherman, K. Lee, J. Leib, A. Madhavan, and K. Marla, "A 10nm high performance and low-power CMOS technology featuring 3rd generation FinFET transistors, Self-Aligned Quad Patterning, contact over active gate and cobalt local interconnects," in *IEDM Tech Dig.*, Dec 2017, pp. 29.1.1-29.1.4, doi: 10.1109/IEDM.2017.8268472.
- [8] IRDS 2018 Edition, 2018. [<https://irds.ieee.org/editions/2018>]
- [9] D. Kwon, S. Cheema, Y. Lin, Y. Liao, K. Chatterjee, A. Tan, C. Hu, S. Salahuddin, "Near Threshold Capacitance Matching in a Negative Capacitance FET With 1 nm Effective Oxide Thickness Gate Stack," in *IEEE Electron Device Letters*, vol. 41, no. 1, pp. 179-182, Jan. 2020, doi: 10.1109/LED.2019.2951705.
- [10] M. Hoffmann, M. Pestic, S. Slesazech, U. Schroeder, and T. Mikolajick, "On the stabilization of ferroelectric negative capacitance in nanoscale devices," *Nanoscale*, no. 23, pp. 10891-10899, May 2018, doi: 10.1039/C8NR02752H.
- [11] G.-M. Rignanes, X. Gonze, G. Jun, K. Cho, and A. Pasquarello, "First-principles investigation of high-K dielectrics: Comparison between the silicates and oxides of hafnium and zirconium," *Phys. Rev. B*, vol. 69, p. 184301, May 2004. doi: 10.1103/PhysRevB.69.184301
- [12] X. Zhao, D. Ceresoli, and D. Vanderbilt, "Structural, electronic, and dielectric properties of amorphous ZrO2 from ab initio molecular dynamics," *Phys. Rev. B*, vol. 71, p. 085107, Feb 2005. doi: 10.1103/PhysRevB.71.085107
- [13] T.-J. Chen and C.-L. Kuo, "First principles study of the structural, electronic, and dielectric properties of amorphous hfo2," *Journal of Applied Physics*, vol. 110, no. 6, p. 064105, 2011. doi: 10.1063/1.3636362
- [14] D. Fischer and A. Kersch, "The effect of dopants on the dielectric constant of hfo2 and zro2 from first principles," *Applied Physics Letters*, vol. 92, no. 1, p. 012908, 2008. doi: 10.1063/1.2828696
- [15] G. Dutta, K. P. S. S. Hembram, G. M. Rao, and U. V. Waghmare, "Effects of o vacancies and c doping on dielectric properties of zro2: A first-principles study," *Applied Physics Letters*, vol. 89, no. 20, p. 202904, 2006. doi: 10.1063/1.2388146
- [16] Y. Liao, D. Kwon, S. Cheema, A. Tan, M. Kao, L. Wang, C. Hu, and S. Salahuddin, "Anomalous Subthreshold Behaviors in Negative Capacitance Transistors," Jun. 2020. [Online]. Available: <https://arxiv.org/abs/2006.02594v1>
- [17] Y.-H. Liao, D. Kwon, Y.-K. Lin, A. J. Tan, C. Hu, S. Salahuddin, "Anomalous Beneficial Gate-Length Scaling Trend of Negative Capacitance Transistors," *IEEE Electron Device Letters*, vol. 40, no. 11, pp. 1860-1863, Nov. 2019, doi: 10.1109/LED.2019.2940715.
- [18] B. K. Kaushik, "Chapter 1 Tunnel FET: Devices and Circuits," in *Nanoelectronics Device, Circuits and Systems 1st ed.*, Dutch: *Elsevier*, 2018, pp. 18-20.
- [19] M.H. Na, E. J. Nowak, W. Haensch, and J. Cai, "The effective drive current in CMOS inverters," in *IEDM Tech Dig.*, Dec. 2012, pp. 121-124, doi: 10.1109/IEDM.2012.1175793.
- [20] H. Agarwal, P. Kushwaha, Y.-K. Lin, M.-Y. Kao, Y.-H. Liao, A. Dasgupta, S. Salahuddin, and C. Hu, "Proposal for Capacitance Matching in Negative Capacitance Field-Effect Transistors," *IEEE Electron Device Letters*, vol. 40, no. 3, pp. 463-466, Mar. 2019, doi: 10.1109/LED.2019.2891540.

[21]M.-Y. Kao, Y.-K. Lin, H. Agarwal, Y.-H. Liao, P. Kushwha, A. Dasgupta, S. Salahuddin, and C. Hu, "Optimization of NCFET by Matching Dielectric and Ferroelectric Nonuniformly Along the Channel," *IEEE Electron Device Letters*, vol. 40, no. 5, pp. 822-825, May 2019, doi: 10.1109/LED.2019.2906314.